Published in final edited form as:
Circ Arrhythm Electrophysiol. 2008 ; 1(3): 209–218. doi:10.1161/CIRCEP.107.748103.

Functional Effects of KCNE3 Mutation and its Role in the Development of Brugada Syndrome

Eva Delpón, PhD[b], **Jonathan M Cordeiro, PhD**[a], **Lucía Núñez, PhD**[b], **Poul Erik Bloch Thomsen, MD**[c], **Alejandra Guerchicoff, PhD**[a], **Guido D. Pollevick, PhD**[a], **Yuesheng Wu, MD**[a], **Jørgen K. Kanters, MD**[c,d], **Carsten Toftager Larsen, MD**[c], **Elena Burashnikov, BS**[a], **Michael Christiansen, MD**[e], and **Charles Antzelevitch, PhD, FAHA**[a]

a*Masonic Medical Research Laboratory, Utica NY*

b*Department of Pharmacology, School of Medicine, Universidad Complutense, Madrid, Spain*

c*Department. of Cardiology P, Gentofte University Hospital, Copenhagen, Denmark*

d*The Danish National Research Foundation Center, Department of Biomedical Sciences, University of Copenhagen, Copenhagen, Denmark*

e*Department of Clinical Biochemistry, Statens Serum Institut, Copenhagen*

Abstract

Introduction—The Brugada Syndrome (BrS), an inherited syndrome associated with a high incidence of sudden cardiac arrest, has been linked to mutations in four different genes leading to a loss of function in sodium and calcium channel activity. Although the transient outward current (I_{to}) is thought to play a prominent role in the expression of the syndrome, mutations in I_{to}-related genes have not been identified as yet.

Methods and Results—One hundred and five probands with BrS were screened for ion channel gene mutations using single strand conformation polymorphism (SSCP) electrophoresis and direct sequencing. A missense mutation (R99H) in *KCNE3* (*MiRP2*) was detected in one proband. The R99H mutation was found 4/4 phenotype positive and 0/3 phenotype-negative family members. Chinese hamster ovary (CHO)-K1 cells were co-transfected using wild-type (WT) or mutant KCNE3 and either WT KCND3 or KCNQ1. Whole-cell patch clamp studies were performed after 48 hours. Interactions between Kv4.3 and KCNE3 were analyzed in co-immunoprecipitation experiments in human atrial samples. Co-transfection of R99H-*KCNE3* with *KCNQ1* produced no alteration in current magnitude or kinetics. However, co-transfection of R99H *KCNE3* with *KCND3* resulted in a significant increase in the I_{to} intensity compared to WT *KCNE3+KCND3*. Using tissues isolated from left atrial appendages of human hearts, we also demonstrate that $K_V4.3$ and *KCNE3* can be co-immunoprecipitated.

Conclusions—These results provide definitive evidence for a functional role of *KCNE3* in the modulation of I_{to} in the human heart and suggest that mutations in *KCNE3* can underlie the development of BrS.

Corresponding author: Charles Antzelevitch, PhD, FAHA, Executive Director/Director of Research, Gordon K. Moe Scholar, Professor of Pharmacology, Masonic Medical Research Laboratory, 2150 Bleecker Street, Utica, NY 13501-1787, Tel: (315) 735-2217 ext. 117, Fax: (315) 735-5648, E-mail: ca@mmrl.edu.

DISCLOSURES:
Conflict of Interests: None.

Keywords

Genetics; Sudden Cardiac Death; Potassium Channels; Channelopathy; Electrophysiology

INTRODUCTION

The Brugada Syndrome (BrS) is an inherited syndrome characterized by an ST-segment elevation in the right precordial leads (V1-V3) and a high incidence of sudden cardiac arrest. [1] This disorder has been linked to mutations in four different genes leading to a loss of function in sodium and calcium channel activity. Mutations in SCN5A, the α subunit of the sodium channel, were the first to be associated with BrS. [2] Weiss et al. described a second locus on chromosome 3, close to but distinct from SCN5A, linked to the syndrome [3] in a large pedigree in which the syndrome is associated with progressive conduction disease, a low sensitivity to procainamide, and a relatively good prognosis. The gene was recently identified in a preliminary report as the Glycerol-3-Phosphate Dehydrogenase 1-Like Gene (GPD1L) and the mutation in GPD1L was shown to result in a reduction of I_{Na}. [4] The third and fourth genes associated with the BrS were recently identified and shown to encode the α1 (CACNA1C) and β (CACNB2b) subunits of the L-type cardiac calcium channel.[5] Mutations in the α1 and β subunits of the calcium channel were also found to lead to a shorter than normal QT interval, in some cases creating a new clinical entity consisting of a combined Brugada/Short QT syndrome.[5]

Loss of function mutations of sodium and calcium channels associated with BrS are attributable to one of three principal mechanisms : 1) truncation of the ion channel protein yielding a non-functional channel; 2) alteration in channel gating such as changes in activation, inactivation or reactivation kinetics; or 3) altered trafficking of the channels from the endoplasmic reticulum/Golgi complex to the plasma membrane.[6,5]

The typical coved-type ST segment elevation in the electrocardiogram (ECG) is often concealed but can be unmasked by sodium channel blockers and vagal influences.[7] The expression of the phenotype and penetrance of the disease appears to be related to factors that alter the balance of outward and inward currents at the end of phase 1 of the epicardial ventricular action potential. [8] Experimental studies suggest that the presence of a prominent transient outward current (I_{to}) predisposes the myocardium to the development of the BrS by permitting the expression of a prominent phase 1, giving the early phase of the action potential a notched appearance. [9,10, 11] Genes that determine or modulate the expression of I_{to} have long been considered as candidate genes for the development of BrS.[8, 12] Augmentation of I_{to} via mutations that increase the magnitude or alter the kinetics of I_{to} so as to increase total charge, are expected to lead to the development of the BrS.

A calcium-independent I_{to} has been identified in the myocardium of most mammalian species including humans (for reviews see [13,14]), and it is well established that ventricular epicardial tissue has a more prominent I_{to} compared to endocardial tissue. [15-17] In the human ventricles, $K_V4.3$ (encoded by the *KCND3* gene) is the main pore-forming α-subunit of I_{to}.[18] However, currents generated by $K_V4.3$ channels do not recapitulate all the features of the native I_{to}. The electrophysiological properties of $K_V4.3$ channels are modulated by several β-subunits including KChIP2 (K^+-channel interacting protein), which increases peak current density and accelerates recovery from inactivation, [19, 20] and the dipeptidyl-aminopeptidase-like protein (*DPP6*), which has been identified in neuronal and heart tissue and can substantially accelerate inactivation. [21] More recently, it has been demonstrated that KCNE3 β-subunits (encoded by the *KCNE3* gene) can interact with $K_V4.3$ channels,[22] an interaction that decreases the current density.[23] Moreover, it has been demonstrated that the transcription factor *Irx5*, [24] calcineurin

and *NFATc3*[25] contribute to the nonuniform distribution of K_v4 expression, and hence I_{to} function, in the mouse ventricle.

In the present study, we identified a mutation in *KCNE3* in the family of a proband diagnosed with BrS. The effects of these changes in *KCNE3* were studied by heterologous co-expression of *KCNE3* with either $K_v7.1$ (*KvLQT1, KCNQ1*) or $K_v4.3$ channels in Chinese hamster ovary (CHO) K1 cells. When the mutated *KCNE3* was co-transfected with *KCNQ1*, no alteration in the current magnitude or kinetics consistent with the development of BrS was observed. However, co-transfection of the R99H *KCNE3* mutation with *KCND3* resulted in a significant increase in the amplitude of I_{to} compared to WT KCNE3+KCND3. Using tissues isolated from left atrial appendages of human hearts, we further demonstrate that $K_v4.3$ and *KCNE3* can be co-immunoprecipitated. These results provide further evidence for a functional role of *KCNE3* (MiRP2) in the modulation of I_{to} in the human heart and suggest that mutations in KCNE3 can underlie the development of BrS.

METHODS

Mutation screening

The probands screened included 77 males and 28 females, 52 of whom were symptomatic at time of presentation. Seventy one (51 males and 20 females) of the 105 probands displayed a spontaneous Type 1 ST segment elevation in the right precordial leads of the standard ECG. The remainder had a Type 1 ST segment elevation unmasked by raising the position of the right precordial leads by two intercostal spaces or with use of sodium channel blockers. Genetic screening was performed as described previously.[26] Genomic DNA was extracted using QIAamp DNA Blood Mini Kit (QIAGEN, Germany). Polymerase chain reaction (PCR) was used to amplify the DNA fragment corresponding to the single exon of the gene; reactions containing 50 ng genomic DNA and 10 pmol of the appropriate primers were prepared and underwent PCR through 33 cycles at an annealing temperature of 60° C. The PCR product was cleaved by incubating overnight with BstEII in order to obtain two fragments of an appropriate size. SSCP electrophoresis (Single strand conformation polymorphism) of the fragments was performed using GeneGel Excel 12.5/24 kits (Amersham Biosciences AB, Sweden). Aberrant conformers were directly sequenced on a 3100-Avant Genetic analyzer from Applied Biosystems (Foster City, CA) using big dye chemistry. Mutation screening of KCNQ1 and KCNE3 were performed as previously described.[27, 28] The following primers were used for screening of family members: Sense: GAGGTCATTTGAGCTGCAGG; Antisense: CTTGTTGATCTTACAGATAGGG

Cell Transfection/Mutagenesis

Human WT-*KCNE3* and R99H-*KCNE3* were amplified from genomic DNA with primers including the sequences of restriction enzymes: KCNE3F-NheIBglII-GGAAGATCTGCTAGCGCCGCCATGGAGACTACCAATGGAACGGAGAC, KCNE3R-BamHIXhoI CCGCTCGAGGGATCCTTAG**ATC**ATAGACACACGGTTCTTG and KCNE3R-BamHI XhoI-mut CCGCTCGAGGGATCCTTAGATCATCATAGACACATGGTTCTTG. PCR products were then subcloned into pIRES2-Ac GFP1 vector at NheI and BamHI cloning sites. CHO cells were transiently transfected with the cDNA encoding either Kv7.1 (2 μg) and *KCNE3* (1 μg) or Kv4.3 (1.5 μg) and *KCNE3* (1.5 μg) together with the cDNA encoding the CD8 antigen (0.25 μg) by use of FuGENE6 (Roche, Basel Switzerland). Cells were grown on 35mm culture dishes and placed in a temperature-controlled chamber for electrophysiological study (Medical Systems, Greenvale, NY) 2 days post-transfection. Before experimental use, cells were incubated with polystyrene microbeads precoated with anti-CD8 antibody (Dynabeads M450;

Dynal, Norway). Only beaded cells or green beaded cells in case of KCNE3 were used for electrophysiological recording.

Electrophysiology

Voltage clamp recordings from transfected CHO cells were made using patch pipettes fabricated from borosilicate glass capillaries (1.5 mm O.D., Fisher Scientific, Pittsburgh, PA). The pipettes were pulled using a gravity puller (Narashige Corp., Greenvale, NY) and filled with pipette solution of the following composition (mmol/L): 10 KCl, 125 K-aspartate, 1.0 $MgCl_2$, 10 HEPES, 10 NaCl, 5 MgATP and 10 EGTA, pH 7.2 (KOH). The pipette resistance ranged from 1-4 MΩ when filled with the internal solution. The perfusion solution contained (mmol/L): 130 NaCl, 5 KCl, 1.8 $CaCl_2$, 1.0 $MgCl_2$, 2.8 Na acetate, 10 HEPES, pH 7.3 with NaOH. Current signals were recorded using a MultiClamp 700A amplifier (Axon Instruments, Foster City, CA) and series resistance errors were reduced by about 60-70% with electronic compensation. All recordings were made at room temperature. All signals were acquired at 10-50 kHz (Digidata 1322, Axon Instruments, Foster City, CA) with a microcomputer running Clampex 9 software (Axon Instruments, Foster City, CA). Membrane currents were analyzed with Clampfit 9 software.

Co-immunoprecipitation

Left atrial appendage samples were obtained from 5 patients in sinus rhythm undergoing mitral/aortic valve replacement or coronary artery bypass graft surgery. The study was approved by the Ethics Committee of the Hospital Clínico San Carlos and each patient gave written, informed consent. Samples were homogenized with ice-cold sucrose buffer of the following composition: 0.32 mol/L sucrose, 1 mmol/L EDTA, 5 mMTris·HCl, pH 7.4, and a cocktail of protease inhibitors (10 μg/ml 1 leupeptin, 10 μg/ml pepstatin, 1 mmol/L PMSF). For better preserving the putative interaction between Kv4.3 and KCNE3 proteins, the buffer was supplemented with 0.5 mg/ml of freshly prepared 3, 3-dithiobispropionimidate (DTBP, Pierce, Rockford, IL), a thiol-cleavable cross linking agent. [29] The homogenate was centrifuged at 14000 revolutions per minute (rpm) for 40 min. The crude membrane pellet was incubated (1 hr, 4°C) in TNE (50 mmol/L Tris-HCL, pH 7.4, 150 mmol/L NaCl,1 mmol/L EDTA, 0.5 mg/ml DTBP, and protease inhibitors) and solubilized with 1% Triton X-100. Insoluble material was removed by centrifugation at 14000 rpm for 40 min, and the supernatant was used for immunoprecipitation. The solubilized membrane extract (2 mg protein/ml) was precleared with protein A-agarose (Sigma, St. Louis, MO) for 2 h at 4°C. After removing the beads by centrifugation at 14000 rpm for 10 min at 4°C, the extract was incubated (1 h, 4°C) with Kv4.3 antibodies (4 μg, SantaCruz Biotechnology, Santa Cruz, CA). Thereafter, it was incubated overnight with protein A-agarose at 4°C. The samples were centrifuged at 5000 rpm for 15 min at 4°C and the pellet was resuspended with a buffer of the following composition (50 mmol/L Tris-HCL, pH 7.4, 50 mmol/L NaCl, 1 mmol/L EDTA, Triton 1 %). After a subsequent centrifugation (5000 rpm, 15 min at 4°C), the pellet was finally resuspended in Laemmli buffer and heated at 90° C for 3 min. The disulphide linkage in DTBP is cleaved by reduction with 2-mercaptoethanol (10%) present in the loading buffer. Immunoprecipitated proteins were separated in SDS, -polyacrylamide gel electrophoresis (SDS-PAGE, 12%) according to Tutor et al.[30] and transferred to polyvinylidene fluoride membranes (Bio Rad, Hercules, CA). Immunoblots were incubated with the corresponding antibodies to detect each protein. The bound antibodies were detected by chemiluminescence with an ECL detection kit (Amersham Biosciences AB, Sweden). The antibodies used were anti-KCNE3 (1:200, Santa Cruz Biotechnology, Santa Cruz, CA), and the corresponding secondary antibody for Kv4.3 and KCNE3 antibodies (anti-goat, 1:2500, Santa Cruz Biotechnology). Specificity of the Kv4.3 antibody was validated in rat ventricular samples by co-incubating the primary antibody with the antigenic peptide, a strategy that blocked specific bands. Moreover, Western blot lanes of

immunoprecipitation reactions that just include Protein-A without primary antibody excluded non-specific adsorption to the beads.

The selectivity of the Kv4.3 antibody was tested in experiments developed in rat ventricular myocardium (n=6), since Kv4.3 is also expressed in this tissue, and the Santa Cruz antibody (SC-10647) also identifies this protein (only 3 aminoacid difference with the human isoform). For this purpose the specific antigenic peptide used was SC-10647-P (Santa Cruz, ratio Ag:Ab = 20:1). To exclude a non-specific cross linking reaction between KCNE3 and Kv4.3, additional experiments were performed using rat myocardium samples in the absence of crosslinker or in the presence of bis(sulfosuccinimidyl) suberate (BS3, Pierce), a non membrane permeant crosslinker.

Results are presented as Mean ± S.E.M. and n represents the number of cells in each experiment. A Student's t-test or an ANOVA followed by a Student-Newman-Keuls test was used where appropriate for comparing paired data and a $p<0.05$ value was considered statistically significant.

The authors had full access to and take full responsibility for the integrity of the data. All authors have read and agree to the manuscript as written.

RESULTS

An R99H missense mutation in *KCNE3* (*MiRP2*) was detected in one of our 105 BrS probands. Fig. 1A shows the pedigree of the proband's family illustrating the phenotype-genotype relationships. The proband (II-3, arrow) was asymptomatic until age 36. While resting on a couch, he had a cardiac arrest and was resuscitated. Fig. 1B, recorded a week later, shows a coved-type ST segment elevation (Type I) in leads V1 and V2, and a saddleback ST segment elevation (Type 2) in V3, diagnostic of BrS. Fig. 1C illustrates telemetry lead recordings showing the development of ventricular tachycardia/fibrillation (VT/VF) at night during hospitalization. The proband was implanted with a cardiac defibrillator (ICD) in 1998. A total of 70 appropriate ICD discharges occurred between 1998 and 2005. Fig. 1D shows an example of the onset of VF recorded by the device, displaying frequent closely-coupled extrasystoles, the third of which precipitated VT/VF. In August of 2005, ablation of the right ventricular outflow tract (RVOT) was performed; over the following 22 month follow-up period, only one additional appropriate ICD shock was delivered.

Fig. 1E shows an electrocardiogram (ECG) of the proband's asymptomatic brother, displaying a coved-type ST segment elevation in V1 and V2. He was also implanted with an ICD which has not discharged as yet. III-1 and III-4 were clinically negative when first examined at ages 13 and 8, respectively. They underwent a sodium block challenge with ajmaline at that time, which was negative in both. A sodium challenge with flecainide was repeated nearly 10 years later, when they were 23 and 18, respectively. The test now showed ST segment elevation in the right precordial leads in both. In the case of III-1, the ECG after flecainide was typical of BrS, whereas in the case of III-4, the youngest member of the family, the ECG displayed an ST segment in V2 and a very prominent exaggeration of the R wave (J wave) in lead aVR, consistent with the recent report of Bigi et al. [31], who identified this change in aVR as a risk factor for development of life-threatening cardiac events in patients with BrS. Their baseline ECGs also displayed an ST segment elevation at this age, particularly when the V1 and V2 leads were raised 2 intercostal spaces. The father of the proband was not a carrier and was clinically negative and the mother, the presumed carrier of the genetic mutation, died from cancer at an early age. The wives of the proband and his brother (II-1 and II-4) were not genetically tested because they are obligate wild-type carriers. Thus, all phenotypically-positive members of the family were positive for the R99H missense mutation in *KCNE3*.

Table 1 shows the clinical ECG characteristics for each of the family members. I-1, II-1 and II-4 were diagnosed as unaffected by their cardiologists 10 years ago, but their ECGs are not available. All parameters were within normal limits, with the exception of ST segment voltage, which was elevated in all family members carrying the R99H mutation.

Since loss-of-function of the cardiac sodium channel gene (SCN5A) has been implicated as a cause of the BrS, we initially screened the blood of the affected individuals for mutations in SCN5A. No mutations or polymorphisms in SCN5A were detected. We sequentially screened SCN5A, KCNQ1, KCNH2, KCNE1, KCNE2, KCNE3, KCNE4, KCNE5, CACNA1C, CACNB2b, GPD1L, KCND3 (Kv4.3), KCHiP2 and SCN1B. We only detected a nucleotide variation in KCNE3 (CGT turns into CAT) predicting a substitution of a histidine for an arginine at position 99 (R99H). All phenotypically-positive members of the family were positive for the R99H mutation in *KCNE3*. The variation was not found in 200 ethnically-matched alleles (Danish individuals) or in an additional 206 alleles of Caucasian controls of European origin. SCN5A mutations were detected in 14.3%, CACNA1C in 6.7% and CACNB2b in 4.8% of the 105 BrS probands studied.

With a screen of 406 control alleles, we were able to exclude with high probability the likelihood that the mutation is a common polymorphism in the population. The upper bound on the frequency of this allele in the general population is 0.0090448 (97.5% upper one-side confidence bound), calculated using STATA Version 10.0. (Stata Corporation, TX).

An interaction of SCN5A and *KCNE3* has not been reported in the literature, however, previous studies have demonstrated that KCNE3 can interact with Kv7.1 channels to produce a current that exhibits rapid activation and decay kinetics.[32, 33] To determine if the R99H mutation results in an alteration of Kv7.1+KCNE3 current, we transiently transfected plasmids encoding the mutant KCNE3 subunit together with Kv7.1 channels. Fig. 2A shows Kv7.1+*KCNE3* currents elicited by 2 s pulses from -80 to +60 mV. The current activated rapidly, reached a maximum (τ_{act}=29.7±2.2 ms at +60 mV, n=11) (Fig. 2E) and did not exhibit further increase or decrease during the application of the depolarizing pulse. Tail currents elicited upon return to -40 mV were well fit by a monoexponential function (τ_{deact}=34.4±4.6 ms after pulses to +60 mV, n=8) (Fig. 2F). Fig. 2B shows Kv7.1+*KCNE3* R99H current. The R99H mutation produced currents that activated significantly slower (Fig. 2E), but with similar deactivation kinetics (Fig. 2F) compared with *KCNE3* WT.

Fig. 2C shows the current-voltage relationships and, Fig. 2D the activation curves constructed by plotting tail current amplitudes recorded on return to -40 mV as a function of the membrane potential of the preceding pulse. Kv7.1+*KCNE3* R99H produced a significantly lower current density (31.4±8.2 pA/pF at +60 mV, n=8, vs. 94.1±19.4 pA/pF, n=11, $P<0.01$) than Kv7.1 +*KCNE3* WT. The R99H mutation displayed a smaller tail current amplitude at potentials positive to 20 mV (7.3±1.9 pA/pF after pulses to +60 mV, n=8, vs. 16.6±4.2 pA/pF, n=11, $P<0.05$), and shifted the midpoint of the activation curve (V_h) to more positive potentials (110.8 ±24.4 mV vs 61.2±5.9 mV, n=6, $P<0.05$), without modifying the slope (10.5±1.9 mV). Tail currents elicited with depolarization to +20 mV, the normal plateau potential of the ventricular action potential, were not significantly reduced. It was clear that these effects of R99H could not account for the BrS phenotype of the patients.

Because a more prominent transient outward current (I_{to}) is thought to underlie the development of the Brugada phenotype,[10,8] we considered the hypothesis that the mutated *KCNE3* subunit may be interacting with Kv4.3 channels to enhance I_{to} and thus predispose to the development of BrS. We co-expressed Kv4.3 alone or together with WT-*KCNE3* (Fig. 3). Voltage steps from -50 to +50 mV applied to the Kv4.3 transfected cells elicited a rapidly inactivating component and a small sustained component (Fig. 3A). Co-transfection of Kv4.3

and WT *KCNE3* resulted in a dramatic reduction in $I_{Kv4.3}$ (Panels B and C in Fig. 3), consistent with earlier observations that heterologous expression of *KCNE3* can interact with Kv4.3 to reduce the magnitude of the current.[23]

We next examined the effect of the R99H-*KCNE3* on $I_{Kv4.3}$ magnitude. Fig. 4A and B shows families of current traces generated by channels formed by *Kv4.3+KCNE3* WT and Kv4.3 +R99H-*KCNE3* channels, respectively. Co-transfection with the R99H mutant resulted in a larger current (Fig. 4B). Analysis of the current-voltage relationship of peak $I_{Kv4.3}$ showed that the current density was significantly greater at potentials positive to -20 mV (52.6±15 pA/pF at +50 mV vs. 18.3±4.6 pA/pF, n=9, P<0.01) (Fig. 4C).

We next assessed whether the difference in current density produced by the co-expression of WT or mutated *KCNE3* with Kv4.3 was due to alterations in steady-state gating parameters. Steady-state inactivation of I_{to} was evaluated using a standard prepulse-test pulse voltage clamp protocol (top inset of Fig. 4). The peak current following a 500 ms prepulse was determined and plotted as a function of the prepulse voltage. The inactivation parameters were obtained by fitting a Boltzmann function to the data (Fig. 4D). Co-expression of *KCNE3* WT (-28.2±2.5 mV, n=9) or R99H (-32.3±2.2 mV, n=8) with *Kv4.3* subunits did not significantly modify the mid-inactivation (V_h) voltage of *Kv4.3* channels (-31.7±1.2 mV, n=16, P>0.05). These results suggest that both the decrease in current density produced in the presence of WT-*KCNE3* or the increase produced by R99H cannot be accounted by a shift in the voltage-dependence of inactivation of the channels.

We also analyzed the inactivation kinetics of *Kv4.3* currents and their possible modification by co-expression with WT-*KCNE3* or R99H-*KCNE3*. A mono-exponential function was fitted to the current decay of traces elicited by pulses positive to -10 mV. Fig. 5 shows mean data showing inactivation time constants for $I_{Kv4.3}$ at various potentials. Kv4.3 channel inactivation kinetics were faster at the more positive potentials (τ decreased from 97.7±12.9 ms at 0 mV to 56.4±4.8 ms at +50 mV (p<0.01, n=10). Co-expression of WT-*KCNE3* produced a significant slowing of the inactivation process as reflected by the marked increase in time constant at all the potentials tested (p<0.01). Inactivation kinetics were faster with the R99H-*KCNE3* mutation compared to WT (τ at +50 mV decreased from 92.3±10.4 to 58.4±5.6 ms, n=10, p<0.01).

Because the R99H mutation produced both an increase in peak current and an acceleration of inactivation, we calculated the total charge contributing to the early phases of the action potential. The charge was calculated by integrating the first 40 ms of the current elicited by pulses positive to -10 mV. Fig. 5B shows a significant increase in total charge when R99H- vs. WT-*KCNE3* is co-expressed with *Kv4.3*.

Because I_{to} magnitude can be influenced by changes in the time course of reactivation,[34, 35] we evaluated the effect of WT- and R99H-*KCNE3* on recovery of $I_{Kv4.3}$ from inactivation by applying twin pulses of 500 ms duration to +50 mV with a variable interpulse interval (Fig. 6). Reactivation of $I_{Kv4.3}$ at -80 mV was monoexponential with a τ of 198.3±37.2 ms. Co-expression of WT- and R99H-*KCNE3* did not modify the recovery process (τ of 181.6±12.0 and 181.0±47.4 ms, respectively, Fig. 6C).

Next we assessed whether the combined presence of WT- and R99H-*KCNE3* produces the same effects on $I_{Kv4.3}$ as R99H-*KCNE3* alone. For this purpose cells were transfected with Kv4.3 encoding gene (1.5 μg) as well as with WT-*KCNE3* and R99H-*KCNE3* (0.75 μg of each one). Fig. 7 summarizes the results obtained in this group of experiments demonstrating that the presence of WT-*KCNE3* and R99H-*KCNE3* significantly increased the peak current density similarly as R99H-*KCNE3* alone did (Panel A). Those Kv4.3 channels co-expressed with WT and R99H-*KCNE3* subunits also exhibited an inactivation kinetics significantly faster than

those co-expressed with WT-*KCNE3* alone (τ at +50 mV 47.9±4.6 ms, n=8, p<0.01). However, in spite of the acceleration of the inactivation kinetics, the combined presence of WT and R99H-*KCNE3* together with Kv4.3 subunits produced a significant increase in total charge crossing the membrane calculated as the current time integral (Fig. 7B). Finally, the presence of WT and R99H-*KCNE3* (Vh= -40.7±2.2 mV) did not modify the voltage-dependence of either Kv4.3 +WT-*KCNE3* (-39.3±0.7 mV) or Kv4.3+R99H-*KCNE3* (-40.5±0.3 mV) (Fig. 7C). While our results provide evidence in support of an important influence of *KCNE3* on the kinetics and magnitude of *Kv4.3* current expressed in CHO cells, it remains unclear whether the *KCNE3* subunits play a functional role in modulation of native I_{to} in the human heart. To determine whether *KCNE3* proteins associate with Kv4.3 in the human myocardium, we prepared extracts of left human atrial appendages (5 patients), and immunoprecipitated them with human anti-Kv4.3 antibodies and protein A beads, followed by separation by SDS-PAGE, and transfer to membranes. Fig. 8 pictures Western blots of the immunoprecipitated proteins showing a ~80 kDa Kv4.3 band detected using the anti-Kv4.3 antibody. In the same immunoprecipitated proteins (IPP) use of an anti-KCNE3 antibody identified a *KCNE3* band of ~30 kDa. Fig. 8 also show that both anti-Kv4.3 and anti-KCNE3 antibodies failed to detect any band in the supernatant (SN) obtained during the immunoprecipitation with Kv4.3 antibody. These results provide evidence in support of an association of subsidiary *KCNE3* subunits with Kv4.3 α subunits in the in human heart. W**e** additionally tested the specificity of the Kv4.3 antibody used. These experiments were developed in rat ventricular myocardium (n=6), since Kv4.3 is also expressed in this tissue, and the antibody also identifies this protein (only 3 aminoacids of difference with the human isoform). A sample was treated with the antibody following identical procedure used with the human samples (2 μg per 500 μg of total protein) (lane 2). Another sample was exposed to the antibody after incubating it with the antigenic peptide (ratio Ag:Ab = 20:1) (lane 3). Another rat myocardium sample was treated only with protein A-agarose (lane 4) without adding antibody. Finally, as another negative control, untransfected CHO cells were used (lane 1). As can be observed (Fig. 8B) the band was present only in lane 2 demonstrating the specificity of the Kv4.3 antibody. In another set of experiments the co-immunoprecipitation in rat ventricular myocardium was tested. Rat samples were prepared following the same procedure used for human atrial samples. Lane 4 (figure 8C) was obtained when using DTBP as crosslinker for better preserving the putative Kv4.3 and *KCNE3* interaction (see methods). The same results were obtained when a non-permeant crosslinker was used (BS3, lane 5), and when no crosslinker was added (lanes 2 and 3). In the latter case, the intensity of the KCNE3 bands was somewhat less even when the total protein charged was doubled. Finally, lane 1 shows that no band was observed with untransfected CHO cells. Therefore, we also observed that association of Kv4.3 and KCNE3 is produced in the rat ventricular myocardium even in the absence of crosslinker which excludes a non-specific cross linking reaction between *KCNE3* and Kv4.3.

DISCUSSION

To our knowledge, this is the first report of a family of BrS in which the disease phenotype is observed as a result of a mutation in a gene affecting I_{to}. Our genetic screen identified the same missense mutation (R99H) in KCNE3 in all clinically affected members of the BrS family, but not in ethnically matched controls. An arginine at codon 99 (R99) of KCNE3 is highly conserved among species.

Our results demonstrate that *KCNE3* β subunits can interact with both Kv7.1 and Kv4.3 channels. WT *KCNE3* subunits interact with Kv7.1 to produce an acceleration of the activation and decay of this current. Co-transfection with R99H-*KCNE3* slowed activation kinetics relative to the WT and reduced current amplitude at positive potentials. However, $I_{Kv7.1}$ tail currents were not significantly affected at the normal plateau potentials of the ventricular action potential. These results suggest that interaction of the mutant *KCNE3* subunit with Kv7.1

channels is unlikely to contribute to development of the phenotype in this BrS family. We also demonstrate that the *KCNE3* subsidiary subunit interacts with Kv4.3 to produce a reduction in the magnitude of $I_{Kv4.3}$. The R99H *KCNE3* mutation reverses the suppression of Kv4.3 channel function, producing a statistically significant increase in the magnitude and kinetics of $I_{Kv4.3}$. Interestingly, the gain of function caused by the mutant β subunit demonstrated a positive dominant effect, since the increase in Kv4.3 current was comparable in the combined presence of WT and R99H *KCNE3* as with R99H *KCNE3* alone. This gain of function in I_{to} is expected to predispose to the development of the BrS phenotype.[8, 10] Finally, using co-immunoprecipitation techniques, we demonstrate that Kv4.3 and *KCNE3* co-associate in the human heart, suggesting that this interaction is important to the functional regulation of I_{to} by this subsidiary subunit.

The Contribution of R99H *KCNE3* Mutation to the Electrocardiographic and Arrhythmic Manifestation of BrS

Patch clamp analysis of WT *KCNE3* interaction with Kv7.1 demonstrates that this ancillary subunit produces a substantial increase in the activation rate as well as a faster decay of the tail current, consistent with previously published results.[32, 33] However, co-transfection of the R99H-*KCNE3* mutation did not alter the magnitude or kinetics of delayed rectifier current (I_{Ks}) current at potentials consistent with the action potential, indicating that alteration of this current is not responsible for the development of the BrS phenotype.

A recent study showed that co-expression of *KCNE3* with Kv4.3 in Xenopus oocytes results in a reduction in $I_{Kv4.3}$ compared to expression of Kv4.3 alone.[23] Co-expression of *KCNE3* with Kv4.3 in our mammalian cell line caused a similar reduction in $I_{Kv4.3}$. The R99H mutation in *KCNE3* reversed this effect of the subsidiary subunit, pointing to the ability of the mutation to cause a gain of function in I_{to}. The electrocardiographic and arrhythmic manifestation of BrS are thought to be due to amplification of intrinsic heterogeneities in the early phases of the action potential among epi-, mid- and endocardial cells, particularly in the right ventricle.[8, 36] In BrS, a decrease in inward currents such as I_{Na} or I_{Ca} or an increase in one of the repolarizing currents active during phase 1 of the action potential, particularly I_{to}, can accentuate the spike-and-dome morphology of the epicardial action potential, giving rise to a down-sloping ST segment elevation with a negative T wave, the typical BrS ECG. A further outward shift in the balance of current can lead to loss of the action potential dome, creating both a transmural and epicardial dispersion of repolarization. The transmural dispersion gives rise to an ST segment elevation, creating a vulnerable window across the ventricular wall, whereas the epicardial dispersion of repolarization gives rise to a phase 2 reentrant extrasystole that captures the vulnerable window to precipitate a rapid polymorphic VT in the form of reentry.

I_{to} levels play a pivotal role in the manifestation of the syndrome and a lower intensity of the current in females is thought to protect them from the arrhythmic consequence of the inherited genetic defects responsible for BrS.[10] Although genes that modulate I_{to} have long been considered candidate genes for the disease,[37] until this report, none have been uncovered. One possible explanation is that gain of function mutations in I_{to} are likely to be lethal *in utero*. A minor slowing of the inactivation kinetics of the current can give rise to a dramatic increase in total charge causing marked abbreviation of the action potential throughout much of the myocardium, thus leading to contractile failure. The R99H mutation in *KCNE3* leads to a very significant increase in peak current density, as well as an acceleration of inactivation kinetics, so that total charge increases only modestly.

ACKNOWLEDGEMENTS

We thank Dr. A. López Farré for his helpful suggestions.

FUNDING SOURCES:

This work was supported by grants from the American Health Assistance Foundation (JMC), by grant HL47678 from NHLBI (CA), grants SAF2005/04609, PR-2005-0058, and RED HERACLES (RD06/0009/0014) (ED) and NYS and Florida Grand Lodges F. & A.M.

Reference List

1. Brugada P, Brugada J. Right bundle branch block, persistent ST segment elevation and sudden cardiac death: a distinct clinical and electrocardiographic syndrome: a multicenter report. J Am Coll Cardiol 1992;20:1391–1396. [PubMed: 1309182]
2. Chen Q, Kirsch GE, Zhang D, Brugada R, Brugada J, Brugada P, Potenza D, Moya A, Borggrefe M, Breithardt G, Ortiz-Lopez R, Wang Z, Antzelevitch C, O'Brien RE, Schultze-Bahr E, Keating MT, Towbin JA, Wang Q. Genetic basis and molecular mechanisms for idiopathic ventricular fibrillation. Nature 1998;392:293–296. [PubMed: 9521325]
3. Weiss R, Barmada MM, Nguyen T, Seibel JS, Cavlovich D, Kornblit CA, Angelilli A, Villanueva F, McNamara DM, London B. Clinical and molecular heterogeneity in the Brugada syndrome. A novel gene locus on chromosome 3. Circulation 2002;105:707–713. [PubMed: 11839626]
4. London B, Michalec M, Mehdi H, Zhu X, Kerchner L, Sanyal S, Viswanathan PC, Pfahnl AE, Shang LL, Madhusudanan M, Baty CJ, Lagana S, Aleong R, Gutmann R, Ackerman MJ, McNamara DM, Weiss R, Dudley SC Jr. Mutation in glycerol-3-phosphate dehydrogenase 1 like gene (GPD1-L) decreases cardiac Na+ current and causes inherited arrhythmias. Circulation 2007;116:2260–2268. [PubMed: 17967977]
5. Antzelevitch C, Pollevick GD, Cordeiro JM, Casis O, Sanguinetti MC, Aizawa Y, Guerchicoff A, Pfeiffer R, Oliva A, Wollnik B, Gelber P, Bonaros EP Jr. Burashnikov E, Wu Y, Sargent JD, Schickel S, Oberheiden R, Bhatia A, Hsu LF, Haissaguerre M, Schimpf R, Borggrefe M, Wolpert C. Loss-of-function mutations in the cardiac calcium channel underlie a new clinical entity characterized by ST-segment elevation, short QT intervals, and sudden cardiac death. Circulation 2007;115:442–449. [PubMed: 17224476]
6. Baroudi G, Pouliot V, Denjoy I, Guicheney P, Shrier A, Chahine M. Novel mechanism for Brugada syndrome: defective surface localization of an SCN5A mutant (R1432G). Circ Res 2001;88:E78–E83. [PubMed: 11420310]
7. Antzelevitch, C.; Brugada, P.; Brugada, J.; Brugada, R. The Brugada Syndrome: From Bench to Bedside. Blackwell Futura; Oxford: 2005.
8. Antzelevitch C. Brugada syndrome. PACE 2006;29:1130–1159. [PubMed: 17038146]
9. Yan GX, Antzelevitch C. Cellular basis for the Brugada syndrome and other mechanisms of arrhythmogenesis associated with ST segment elevation. Circulation 1999;100:1660–1666. [PubMed: 10517739]
10. Di Diego JM, Cordeiro JM, Goodrow RJ, Fish JM, Zygmunt AC, Perez GJ, Scornik FS, Antzelevitch C. Ionic and cellular basis for the predominance of the Brugada syndrome phenotype in males. Circulation 2002;106:2004–2011. [PubMed: 12370227]
11. Fish JM, Antzelevitch C. Cellular and Ionic Basis for the Sex-related Difference in the Manifestation of the Brugada Syndrome and Progressive Conduction Disease Phenotypes. J Electrocardiol 2003;36:173–179. [PubMed: 14716629]
12. Antzelevitch C. The Brugada syndrome. J Cardiovasc Electrophysiol 1998;9:513–516. [PubMed: 9607460]
13. Antzelevitch, C.; Dumaine, R. Electrical heterogeneity in the heart: physiological, pharmacological and clinical implications. In: Page, E.; Fozzard, HA.; Solaro, RJ., editors. The Cardiovascular System. Volume 1, The Heart. The American Physiological Society by Oxford University Press; New York: 2002. p. 654-692.
14. Tamargo J, Caballero R, Gomez R, Valenzuela C, Delpon E. Pharmacology of cardiac potassium channels. Cardiovasc Res 2004;62:9–33. [PubMed: 15023549]
15. Litovsky SH, Antzelevitch C. Transient outward current prominent in canine ventricular epicardium but not endocardium. Circ Res 1988;62:116–126. [PubMed: 2826039]

16. Campbell DL, Rasmusson RL, Qu YH, Strauss HC. The calcium-independent transient outward potassium current in isolated ferret right ventricular myocytes. I. Basic characterization and kinetic analysis. J Gen Physiol 1993;101:571–601. [PubMed: 8505627]
17. Fedida D, Giles WR. Regional variations in action potentials and transient outward current in myocytes isolated from rabbit left ventricle. J Physiol 1991;442:191–209. [PubMed: 1665856]
18. Dixon EJ, Shi W, H-S Wang, McDonald C, Yu H, Wymore RS, Cohen IS, McKinnon D. Role of the Kv4.3 K+ channel in ventricular muscle. A molecular correlate for the transient outward current. Circ Res 1996;79:659–668. [PubMed: 8831489]
19. Deschenes I, DiSilvestre D, Juang GJ, Wu RC, An WF, Tomaselli GF. Regulation of Kv4.3 current by KChIP2 splice variants: a component of native cardiac I(to)? Circulation 2002;106:423–429. [PubMed: 12135940]
20. Rosati B, Grau F, Rodriguez S, Li H, Nerbonne JM, McKinnon D. Concordant expression of KChIP2 mRNA, protein and transient outward current throughout the canine ventricle. J Physiol 2003;548:815–822. [PubMed: 12598586]
21. Radicke S, Cotella D, Graf EM, Ravens U, Wettwer E. Expression and function of dipeptidyl-aminopeptidase-like protein 6 as a putative beta-subunit of human cardiac transient outward current encoded by Kv4.3. J Physiol 2005;565:751–756. [PubMed: 15890703]
22. Radicke S, Cotella D, Graf EM, Banse U, Jost N, Varro A, Tseng GN, Ravens U, Wettwer E. Functional modulation of the transient outward current Ito by KCNE beta-subunits and regional distribution in human non-failing and failing hearts. Cardiovasc Res 2006;71:695–703. [PubMed: 16876774]
23. Lundby A, Olesen SP. KCNE3 is an inhibitory subunit of the Kv4.3 potassium channel. Biochem Biophys Res Commun 2006;346:958–967. [PubMed: 16782062]
24. Costantini DL, Arruda EP, Agarwal P, Kim KH, Zhu Y, Zhu W, Lebel M, Cheng CW, Park CY, Pierce SA, Guerchicoff A, Pollevick GD, Chan TY, Kabir MG, Cheng SH, Husain M, Antzelevitch C, Srivastava D, Gross GJ, Hui CC, Backx PH, Bruneau BG. The homeodomain transcription factor Irx5 establishes the Mouse cardiac ventricular repolarization gradient. Cell 2005;123:347–358. [PubMed: 16239150]
25. Rossow CF, Minami E, Chase EG, Murry CE, Santana LF. NFATc3-induced reductions in voltage-gated K+ currents after myocardial infarction. Circ Res 2004;94:1340–1350. [PubMed: 15087419]
26. Hofman-Bang J, Jespersen T, Grunnet M, Larsen LA, Andersen PS, Kanters JK, Kjeldsen K, Christiansen M. Does KCNE5 play a role in long QT syndrome? Clin Chim Acta 2004;345:49–53. [PubMed: 15193977]
27. Larsen LA, Andersen PS, Kanters JK, Jacobsen JR, Vuust J, Christiansen M. A single strand conformation polymorphism/heteroduplex (SSCP/HD) method for detection of mutations in 15 exons of the KVLQT1 gene, associated with long QT syndrome. Clin Chim Acta 1999;280:113–125. [PubMed: 10090529]
28. Larsen LA, Andersen PS, Kanters J, Svendsen IH, Jacobsen JR, Vuust J, Wettrell G, Tranebjaerg L, Bathen J, Christiansen M. Screening for mutations and polymorphisms in the genes KCNH2 and KCNE2 encoding the cardiac HERG/MiRP1 ion channel: implications for acquired and congenital long Q-T syndrome. Clin Chem 2001;47:1390–1395. [PubMed: 11468227]
29. Nadal MS, Ozaita A, Amarillo Y, Vega-Saenz de ME, Ma Y, Mo W, Goldberg EM, Misumi Y, Ikehara Y, Neubert TA, Rudy B. The CD26-related dipeptidyl aminopeptidase-like protein DPPX is a critical component of neuronal A-type K+ channels. Neuron 2003;37:449–461. [PubMed: 12575952]
30. Tutor AS, Delpon E, Caballero R, Gomez R, Nunez L, Vaquero M, Tamargo J, Mayor F Jr. Penela P. Association of 14-3-3 proteins to beta1-adrenergic receptors modulates Kv11.1 K+ channel activity in recombinant systems. Mol Biol Cell 2006;17:4666–4674. [PubMed: 16914520]
31. Babai Bigi MA, Aslani A, Shahrzad S. aVR sign as a risk factor for life-threatening arrhythmic events in patients with Brugada syndrome. Heart Rhythm 2007;4:1009–1012. [PubMed: 17675073]
32. Lundquist AL, Manderfield LJ, Vanoye CG, Rogers CS, Donahue BS, Chang PA, Drinkwater DC, Murray KT, George AL Jr. Expression of multiple KCNE genes in human heart may enable variable modulation of I(Ks). J Mol Cell Cardiol 2005;38:277–287. [PubMed: 15698834]

33. Bendahhou S, Marionneau C, Haurogne K, Larroque MM, Derand R, Szuts V, Escande D, Demolombe S, Barhanin J. In vitro molecular interactions and distribution of KCNE family with KCNQ1 in the human heart. Cardiovasc Res 2005;67:529–538. [PubMed: 16039274]

34. Campbell, DL.; Rasmusson, RL.; Comer, MB.; Strauss, HC. The cardiac calcium-independent transient outward potassium current: kinetics, molecular properties, and role in ventricular repolarization*. In: Zipes, DP.; Jalife, J., editors. Cardiac electrophysiology: From cell to bedside. 2nd ed.. W.B. Saunders; Philadelphia: 1995. p. 83-96.

35. Clark RB, Bouchard RA, Salinas-Stefanon E, Sanchez-Chapula J, Giles WR. Heterogeneity of action potential waveforms and potassium currents in rat ventricle. Cardiovasc Res 1993;27:1795–1799. [PubMed: 8275526]

36. Fish JM, Antzelevitch C. Role of sodium and calcium channel block in unmasking the Brugada syndrome. Heart Rhythm 2004;1:210–217. [PubMed: 15851155]

37. Antzelevitch, C.; Brugada, P.; Brugada, J.; Brugada, R.; Nademanee, K.; Towbin, JA. Clinical Approaches to Tachyarrhythmias. The Brugada Syndrome. Futura Publishing Company, Inc.; Armonk, NY: 1999.

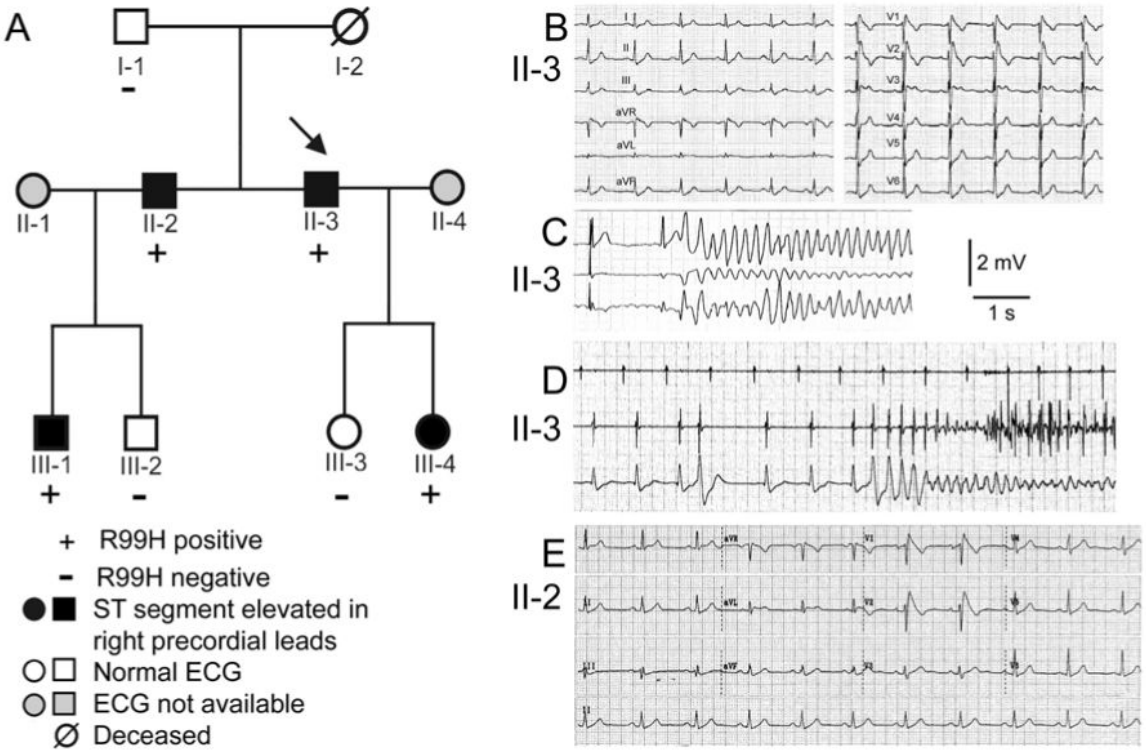

Figure 1.

Pedigree of BrS family (**A**) and ECG recordings of proband and his brother (**B-E**). **B:** 12-lead ECG of 36 year old proband. **C:** ECG of proband recorded using telemetry leads during hospitalization showing initiation of VT. **D:** Initiation of VT recorded by ICD implanted in proband. **E:** 12-lead ECG of brother of proband.

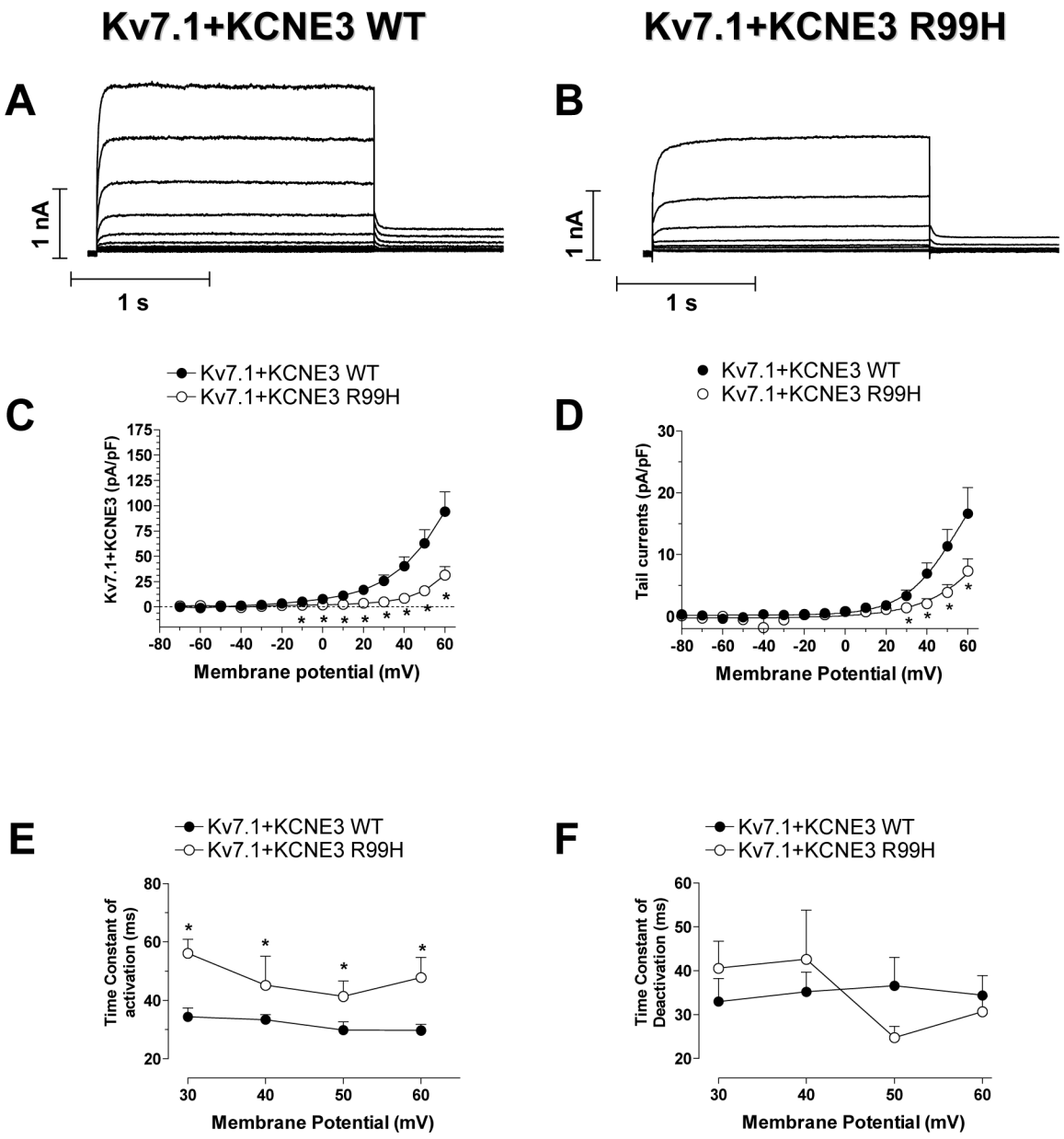

Figure 2.

Representative Kv7.1 currents recorded from CHO-K1 cells co-transfected with WT (**A**) or R99H (**B**) *KCNE3*. Membrane currents were elicited with voltage steps from a -80 mV holding potential to +60 mV. **C-D.** Mean current-voltage relationship for developing currents and tail currents for Kv7.1 channels co-expressed with WT- and R99H-*KCNE3*. In panel D continuous lines represent a Boltzmann function fit to the data. **E-F.** Time constant of activation and deactivation of Kv7.1 channels co-expressed with *KCNE3* WT or R99H. Values in panels **C-F** are Mean±SEM of >8 experiments. * P<0.05 vs. Kv7.1+*KCNE3* data.

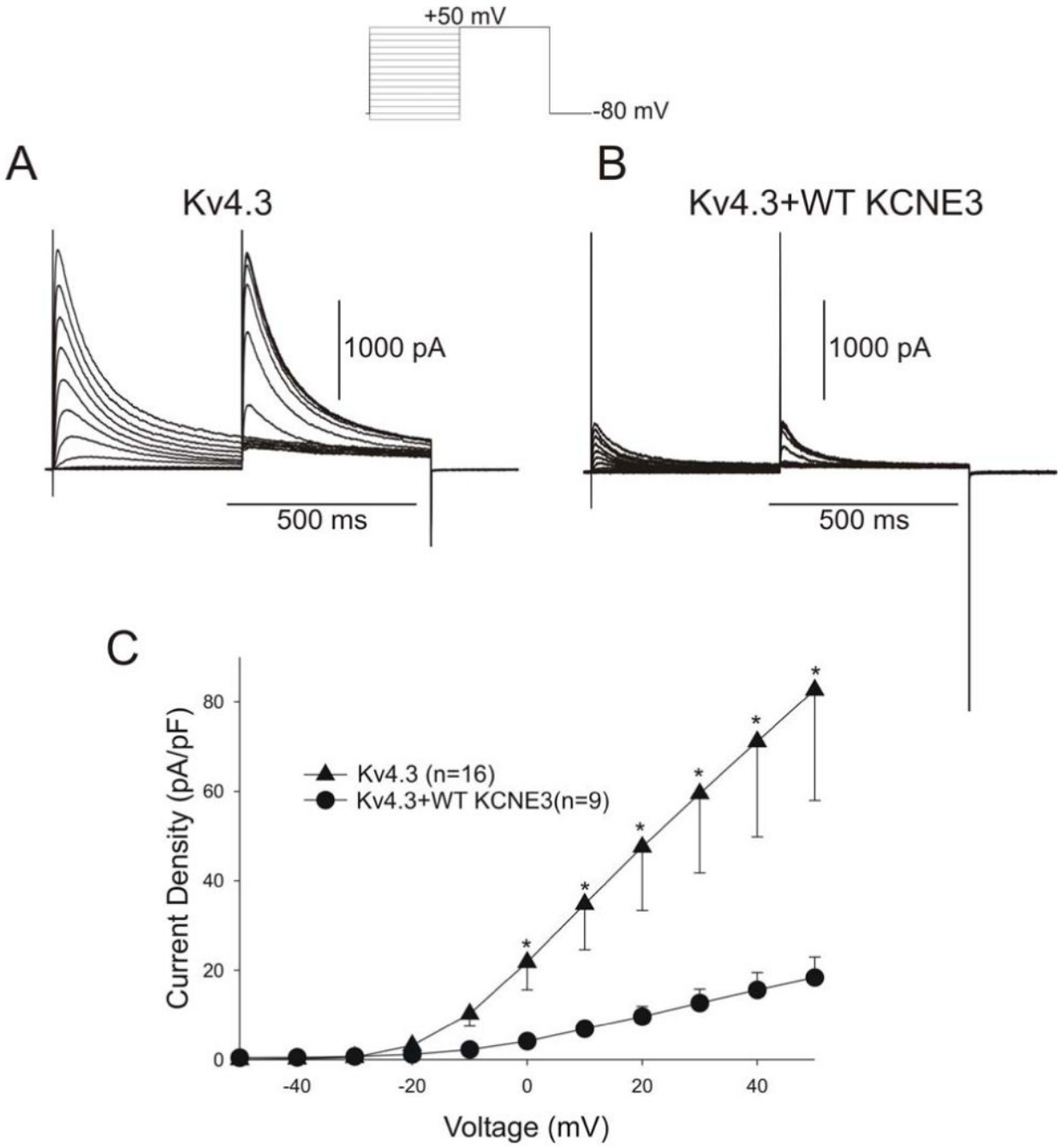

Figure 3.

Representative Kv4.3 currents recorded from CHO-K1 cells in the absence (**A**) and presence (**B**) of ancillary WT-*KCNE3* subunits. Membrane currents were elicited by voltage steps from -80 mV (holding potential) to potentials between -50 and +50 mV. **C:** I-V relation for peak $I_{Kv4.3}$. $I_{Kv4.3}$ density is greater in the absence of WT *KCNE3*. Values shown represent Mean ±SEM. "* P<0.05 vs Kv4.3+WT *KCNE3*.

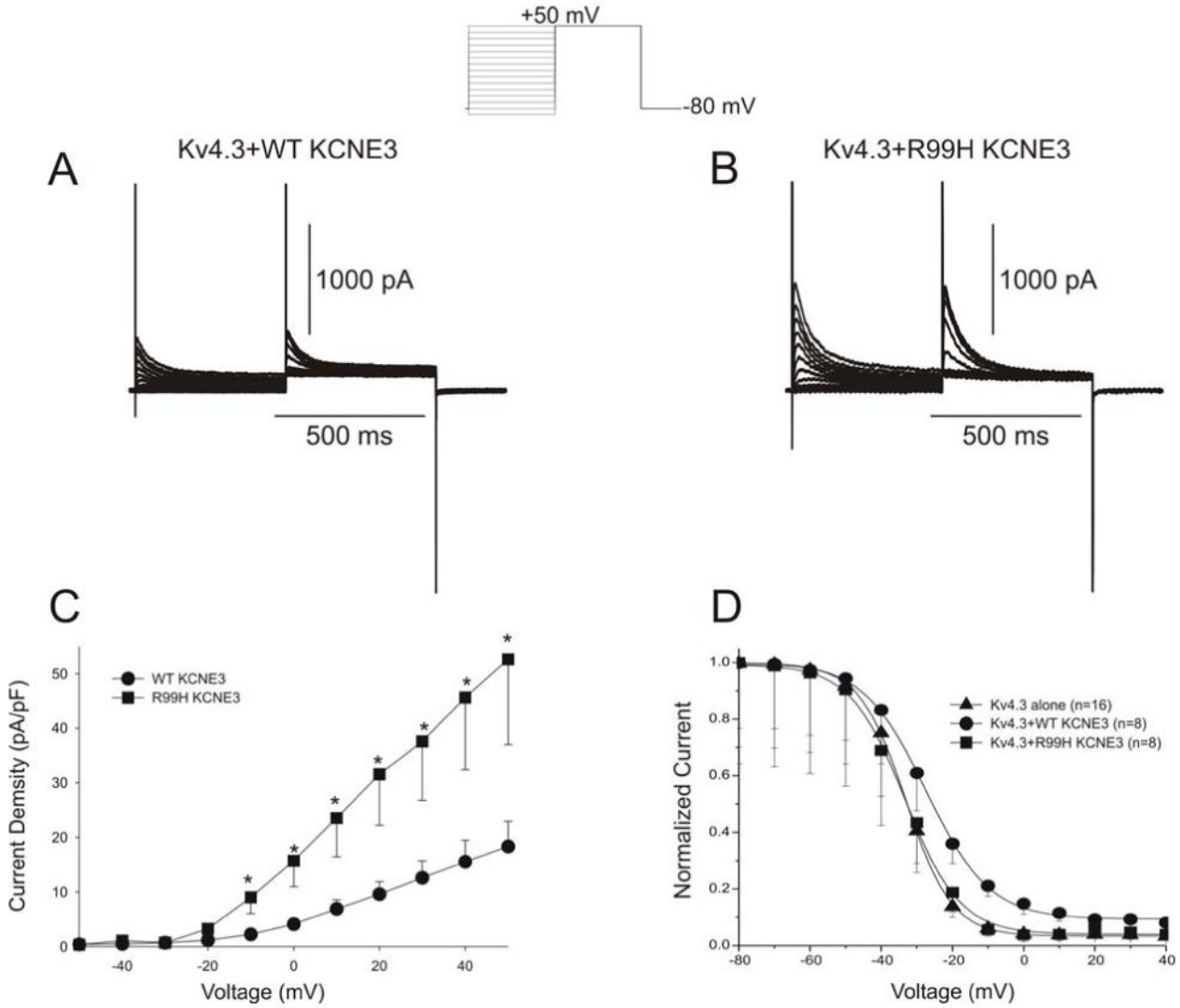

Figure 4.

Representative Kv4.3 currents recorded from CHO-K1 cells co-transfected with either WT **(A)** or R99H **(B)** *KCNE3*. The voltage protocol used is shown in the inset on top. **C:** I-V relation for peak $I_{Kv4.3}$. Average $I_{Kv4.3}$ density is greater in the presence of R99H *KCNE3*. **D:** Steady-state Kv4.3 inactivation curves in the absence and presence of WT- and R99H-*KCNE3*. Continuous lines represent a Boltzmann function fit to the data. Values shown represent Mean ±SEM.

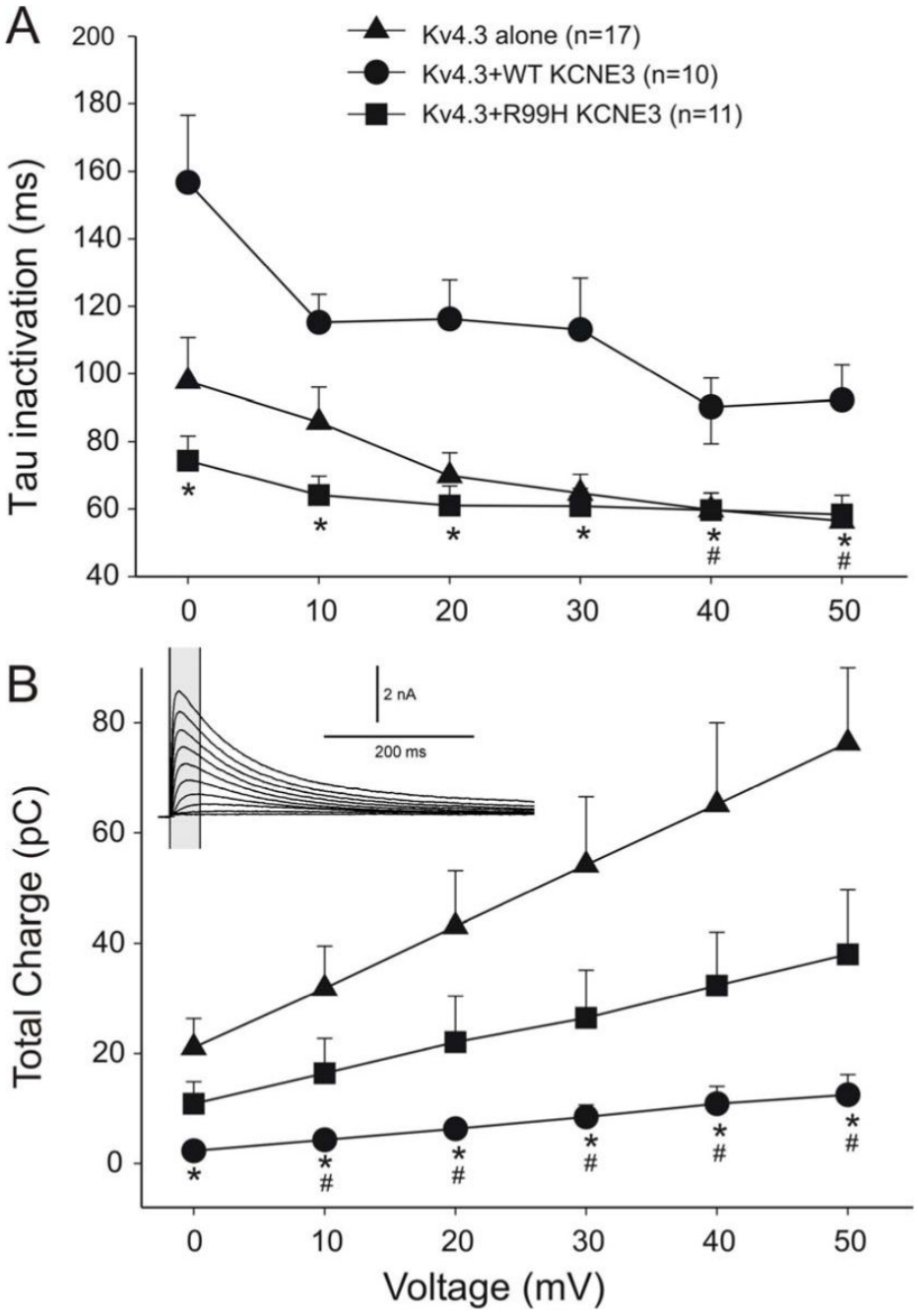

Figure 5.

A: Inactivation time constants (τ) for $I_{Kv4.3}$ as a function of voltage. Values shown represent Mean±SEM. Inactivation time constants values were measured by fitting a monoexponential function to the current decay. *p<0.05 vs Kv4.3+WT KCNE3. #p<0.05 vs Kv4.3+WT KCNE3.
B: Total charge of Kv4.3 during the first 40 ms as a function of voltage. *p<0.05 vs Kv4.3 alone. #p<0.05 vs Kv4.3+R99H KCNE3.

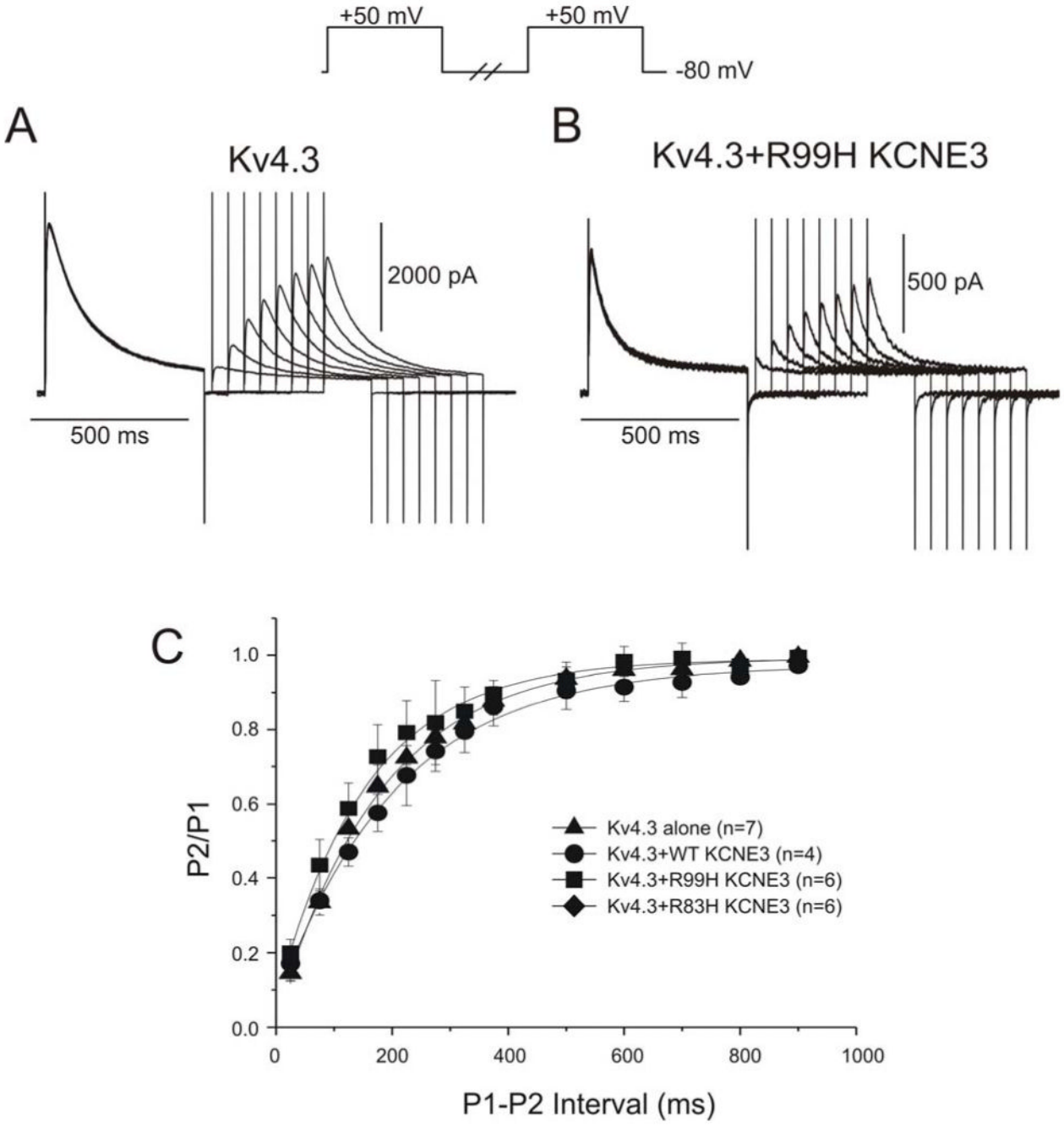

Figure 6.

Representative traces Kv4.3+*KCNE3* (**A**) and Kv4.3+R99H-*KCNE3* currents (**B**) elicited using the protocol shown in the inset. $I_{Kv4.3}$ recovery was measured using twin voltage clamp steps to +50 mV from a holding potential of -80 mV separated by variable time intervals. **(C)** Ratio to peak current amplitude (P2) as a function of the interpulse interval. Values shown represent Mean±SEM.

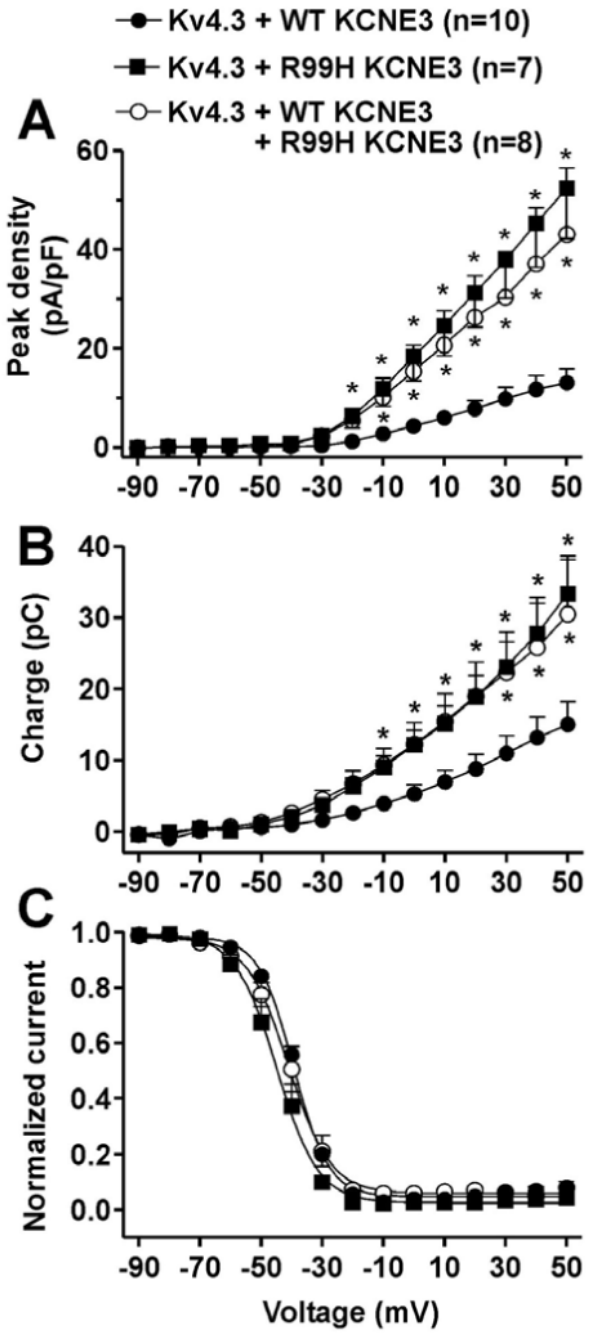

Figure 7.

A: I-V relation for peak $I_{Kv4.3}$ generated by channels formed by the co-expression of Kv4.3 plus WT-*KCNE3*, Kv4.3 plus R99H-*KCNE3*, or Kv4.3 plus WT-*KCNE3* and R99H-*KCNE3*. **B:** Total charge of the current during the first 40 ms as a function of voltage. **C:** Steady-state Kv4.3 inactivation curves in the absence and presence of WT-, R99H-, or WT+R99H-*KCNE3*. Continuous lines represent a Boltzmann function fit to the data. Values shown represent Mean±SEM. * P<0.05 *vs* Kv4.3+WT *KCNE3*.

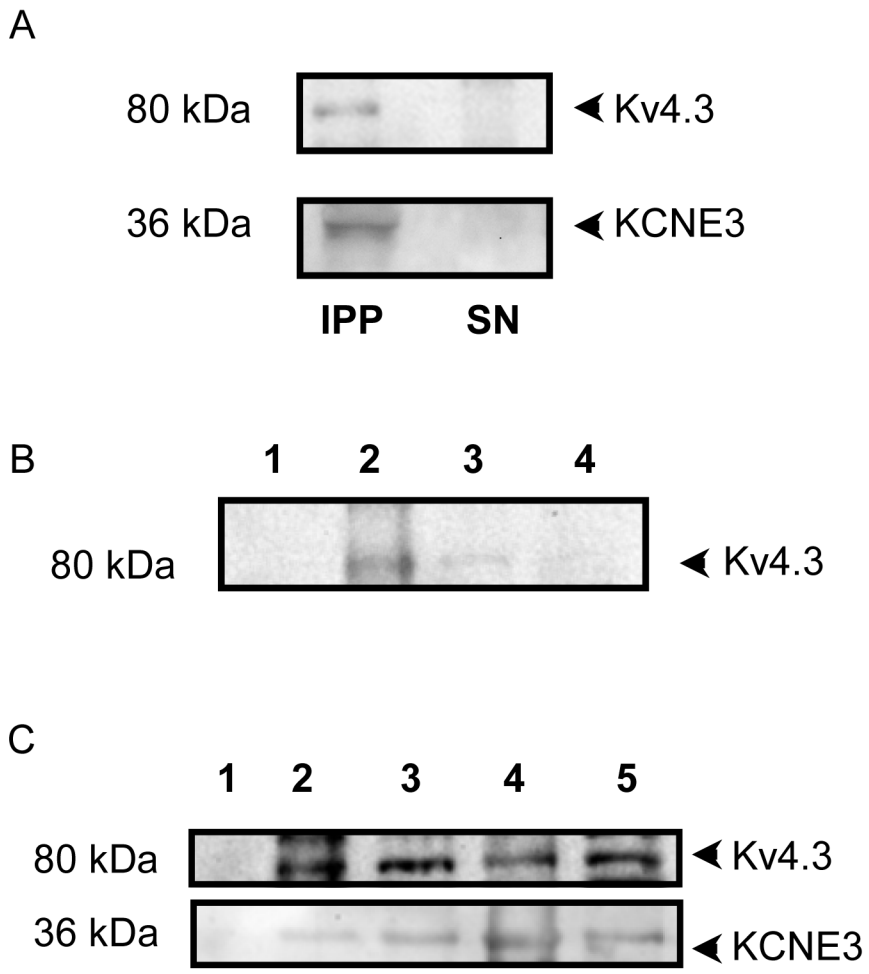

Figure 8.

A: Co-immunoprecipitation of Kv4.3 channel complex with *KCNE3* proteins isolated from human atrial tissues. The blots were probed with anti-Kv4.3 (upper) and anti-*KCNE3* antibody (lower), respectively. IPP: immunoprecipitated proteins, SN: supernatant. **B:** Western blots showing Kv4.3 expression in untransfected CHO cells (lane 1), in rat ventricular myocardium (lane 2), and in rat ventricular myocardium when the sample was exposed to the antibody after incubating it with the antigenic peptide (lane 3) or when it was treated only with protein A-agarose (lane 4). **C**: Co-immunoprecipitation of Kv4.3 channel complex with *KCNE3* proteins isolated from rat ventricular myocardium. The blots were probed with anti-Kv4.3 (upper) and anti-*KCNE3* antibody (lower), respectively. Association of Kv4.3 and *KCNE3* is produced in the absence of crosslinker (lanes 2 and 3), in the presence of DTBP (lane 4) or when a non-permeant crosslinker was used (BS3, lane 5). No bands were observed in the case of untransfected CHO cells (lane 1).

Table 1

Clinical ECG Characteristics

	I-1	II-2	II-3	III-1*	III-2	III-3	III-4*
Age at time of ECG (yrs)	74	46	44	23	8	13	18
Mutation Carrier	-	+	+	+	-	-	+
HR (beats per minute)	88	60	60	65	69	85	90
PQ (ms)	0.19	0.17	0.16	0.22	0.17	0.13	0.19
QT (ms)	0.36	0.39	0.36	0.41	0.37	0.35	0.36
QTc (ms)	0.44	0.39	0.36	0.43	0.40	0.42	0.44
ST elevation (V2) (mV)	0.00	0.41	0.45	0.25	0.07	0.03	0.15
ST elevation + 40 (V2) (mV)	0.05	0.22	0.22	0.22	0.16	0.07	0.23

ST elevation +40 = ST segment elevation measured 40 ms after termination of the QRS

* During Flecainide (2 mg/kg max. 150 mg)